Table 2 Test conditions for data from Refs. 7 and 8

Reference	M_1	Re_x	h_w/h_{aw}	Configuration
7	5.67–7.4	2.5×10^6–6×10^7	0.139–0.142	Flat plate
8	2.5–3.5	10^5–10^6	0.012–0.027	Hollow cylinder

planform loading of 50 lb/ft² is used. The lift coefficient is taken to be Newtonian ($2 \sin^2\alpha\cos\alpha$). For this particular example, transition onset is assumed to occur at a fixed length Reynolds number of 10^6 and fully turbulent flow at 2×10^6. The point of transition onset is taken as a reasonable estimate for the virtual origin of the turbulent boundary layer. Boundary-layer edge conditions are those behind a plane oblique shock and the effect of three-dimensional flow on the centerline heating is approximated by a small correction to the prediction for two-dimensional flow, which accounts for a transverse velocity gradient. The correction increases nearly linearly with angle of attack and amounts to an increase in heating of less than 13% at 50°.

The results are given in terms of the peak radiation equilibrium temperature (emmissivity of 0.85) on the vehicle centerline as a function of angle of attack and are summarized in Fig. 2. It is emphasized that the altitude at peak heating is different for each angle of attack because the equilibrium glide trajectory is different. The altitude of peak heating increases with increasing angle of attack, while the flight velocity for peak heating in fully turbulent flow is essentially constant at about 17,500 fps. These results are shown only to illustrate the different temperature predictions by each method, so the temperature differences rather than the magnitudes are to be emphasized. Spalding and Chi's correlation, which gives the best agreement with experimental data, gives nearly the lowest peak temperature estimates. The difference between the lowest and highest predictions can be greater than 200°F.

The peak temperatures are given in this example for a specific transition criterion and lift coefficient curve in order to show the differences which are obtained by changing only the method for predicting heating in fully turbulent flow. However, it is known that the peak temperature dependence on angle of attack is also very sensitive to the choice of transition criterion and lift coefficient. These are additional factors which can affect the peak temperature predictions by an amount comparable to that of the different heat-transfer prediction methods.

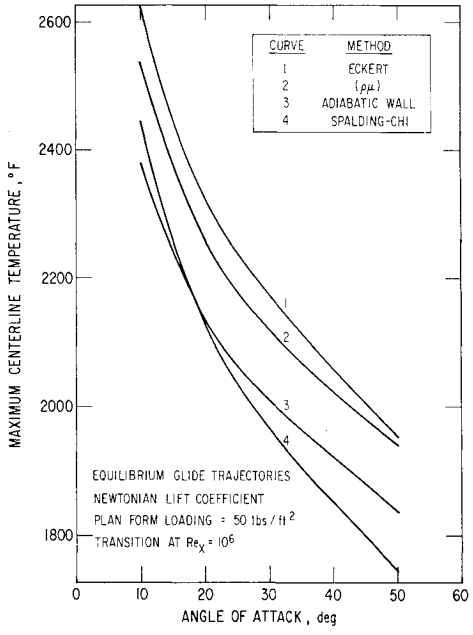

Fig. 2 Maximum centerline radiation equilibrium temperatures (emissivity of 0.85) at peak turbulent heating for a 200-ft, flat delta wing with 80° sweep.

References

[1] Bertram, M. H. and Neal, L., "Recent Experiments in Hypersonic Turbulent Boundary Layers," TM-X-56335, 1965, NASA.

[2] Bertram, M. H., Cary, A. M., and Whitehead, A. H., "Experiments with Hypersonic Turbulent Boundary Layers on Flat Plates and Delta Wings," AGARD Specialists Meeting in Hypersonic Boundary Layers and Flow Fields, London, 1965.

[3] Eckert, E. R. G., "Survey on Heat Transfer at High Speeds," TR 54-70, 1954, Wright Air Development Center, Dayton, Ohio.

[4] Pearce, B. E., "A Comparison of Four Simple Calculation Methods for the Compressible Turbulent Boundary Layer on a Flat Plate," Rept. TOR-0066(5758-02)-3, March 1970, The Aerospace Corp., El Segundo, Calif.

[5] Spalding, D. B. and Chi, S. W., "The Drag of a Compressible Turbulent Boundary Layer on a Smooth Flat Plate With and Without Heat Transfer," *Journal of Fluid Mechanics*, Vol. 18, No. 1, 1964, pp. 117–143.

[6] Savage, R. T. and Jaeck, C. L., "Investigation of Turbulent Heat Transfer at Hypersonic Speeds," AFFDL-TR-67-144, Vol. 1, 1967, Air Force Flight Dynamics Lab., Dayton, Ohio.

[7] Wallace, J. E. and McLaughlin, E. J., "Experimental Investigation of Hypersonic Turbulent Flow and Laminar, Lee-Side Flow on Flat Plates," AFFDL-TR-66-63, Vol. 1, 1963, Air Force Flight Dynamics Lab., Dayton, Ohio.

[8] Hopkins, R. A. and Nerem, R. M., "An Experimental Investigation of Heat Transfer from a Highly Cooled Turbulent Boundary Layer," *AIAA Journal*, Vol. 6, No. 10, Oct. 1968, pp. 1912–1918.

Effect of Suspension Line Elasticity on Parachute Loads

JOHN S. PREISSER* AND GEORGE C. GREENE†
NASA Langley Research Center, Hampton, Va.

Nomenclature

$C_DS(t)$	= instantaneous drag-area of parachute during inflation
C_DS_o	= drag-area of parachute at steady full inflation
$E(t)$	= normalized force, $E = m_2\ddot{x}_2/q_sC_DS_o$
k	= suspension line spring constant (slope of linear approximation to force-elongation curve)
M	= load amplification factor, $M = E_{\max}$
m_1, m_2	= mass of parachute and payload, respectively
n	= exponential power, $n = 1, 2, 3, 4$
q_s	= dynamic pressure at time of snatch force, $q_s = \rho[\dot{x}_1(0)]^2/2$
T	= natural oscillation period of system, $T = 2\pi/\omega$
t	= time from snatch force
t_f	= filling time (from snatch force to full inflation)
$x_1(t), x_2(t)$	= displacement of parachute and payload, respectively
$\xi(t)$	= suspension line elongation, $\xi = x_2 - x_1$
ρ	= atmospheric density
φ	= parameter relating the velocities of m_1 and m_2, $\varphi = (\dot{x}_2/\dot{x}_1) - 1$

Received July 16, 1970.

* Aerospace Engineer. Member AIAA.

† Aerospace Engineer.

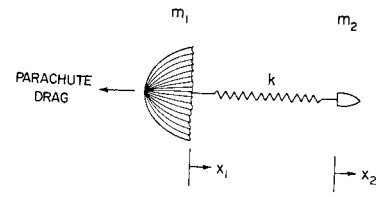

Fig. 1 Elastic parachute system.

τ = dummy variable of integration
ω = natural frequency of system, $\omega = (k/m_2 + k/m_1)^{1/2}$

Introduction

IT is commonly known that the maximum force or opening load associated with the inflation of a parachute at infinite mass conditions is greater than that experienced by a parachute under steady, full inflated conditions at the same dynamic pressure. This increased force or load amplification (usually denoted by the symbol X) has been studied experimentally for specific canopy types.[1] A detailed analysis of load amplification, however, has proven to be intractable, since a parachute is both flexural and porous, and the flowfield about it is rapidly changing during the inflation process.

This Note contains an analysis of parachute loads through the use of a simple model which represents the payload, parachute, and suspension lines by a two-body spring-mass system. This elastic model has previously been used to interpret experimental load histories.[2] The present analysis is intended to emphasize that a significant contribution to the over-all load amplification can result from the elasticity of the parachute suspension lines. In addition, the analysis shows that the atmospheric density is an important factor in determining how effectively load oscillations are damped out following full inflation.

Analysis and Results

A simple mathematical model was constructed in order to analyze the response of the payload to the parachute drag force developed during and immediately following canopy inflation. The model is based on the assumption that the payload-parachute system can be described as point masses joined by elastic parachute suspension lines (which act like a spring) (Fig. 1). The equations of motion for the system may be written as

$$m_1\ddot{x}_1 = -\rho\dot{x}_1^2 C_D S/2 + k(x_2 - x_1),$$
$$m_2\ddot{x}_2 = -k(x_2 - x_1) \quad (1)$$

Gravity has been neglected since it acts uniformly on the entire system. It is also assumed that payload drag is negligible compared to parachute drag, and that internal viscous damping can be ignored.

The dynamic pressure in Eq. (1) can be considered constant during canopy inflation for the infinite mass case, such as in a wind tunnel or for a flight test where the velocity does not appreciably change from snatch force to full inflation.

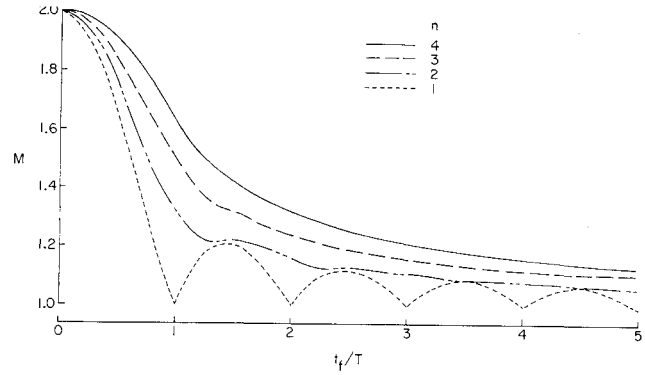

Fig. 2 Load amplification factor, M, for various drag area functions.

During inflation, the increase in drag area, C_DS, can be described by some function of time. Further, the drag area can be nondimensionalized to the fully inflated value of drag area and expressed by the function

$$C_DS/C_DS_o = f(t/t_f)$$

Equations (1) then can be combined to yield

$$\ddot{\xi} + \omega^2\xi = (q_sC_DS_o/m_1)f(t/t_f) \quad (2)$$

This equation represents a simple spring-mass system subject to a time-varying forcing function.

To approximate the range of typically encountered inflation histories one may set $f(t/t_f) = (t/t_f)^n$ for $t \leq t_f$ and $f(t/t_f) = 1$ for $t > t_f$.

To isolate the inflation process from other dynamic effects (such as snatch force), one can choose initial conditions such that there is no relative extension, $\xi(0) = 0$, and no relative velocity, $\dot{\xi}(0) = 0$, at the time of snatch force. The solution to Eq. (2) is given by Duhamel's integral.[3] For $t \leq t_f$,

$$\xi(t) = \frac{q_sC_DS_o}{m_1\omega}\int_0^t \sin\omega(t-\tau)\left(\frac{\tau}{t_f}\right)^n d\tau$$

for the $t > t_f$,

$$\xi(t) = \frac{q_sC_DS_o}{m_1\omega}\int_{t_f}^t \sin\omega(t-\tau)d\tau + \xi(t_f)\cos\omega(t-t_f) + \frac{\dot{\xi}(t_f)}{\omega}\sin\omega(t-t_f) \quad (3)$$

Table 1 Normalized force E for various drag area functions

n	E(for $t \leq t_f$)	E(for $t > t_f$)
1	$\frac{t}{t_f} - \frac{\sin\omega t}{\omega t_f}$	$1 + \frac{1}{\omega t_f}\sin\omega(t-t_f) - \frac{\sin\omega t}{\omega t_f}$
2	$\left(\frac{t}{t_f}\right)^2 - \frac{2}{\omega^2 t_f^2} \quad (1 - \cos\omega t)$	$1 + \frac{2}{\omega t_f}\sin\omega(t-t_f) + \frac{2}{\omega^2 t_f^2}\cos\omega t - \frac{2}{\omega^2 t_f^2}\cos\omega(t-t_f)$
3	$\left(\frac{t}{t_f}\right)^3 - \frac{6}{\omega^3 t_f^3}(\omega t - \sin\omega t)$	$1 + \left(\frac{3}{\omega t_f} - \frac{6}{\omega^3 t_f^3}\right)\sin\omega(t-t_f) + \frac{6}{\omega^3 t_f^3}\sin\omega t - \frac{6}{\omega^2 t_f^2}\cos\omega(t-t_f)$
4	$\left(\frac{t}{t_f}\right)^4 - \frac{24}{\omega^4 t_f^4}\left(\frac{\omega^2 t^2}{2} - 1 + \cos\omega t\right)$	$1 + \left(\frac{4}{\omega t_f} - \frac{24}{\omega^3 t_f^3}\right)\sin\omega(t-t_f) - \frac{24}{\omega^4 t_f^4}\cos\omega t - \left(\frac{12}{\omega^2 t_f^2} - \frac{24}{\omega^4 t_f^4}\right)\cos\omega(t-t_f)$

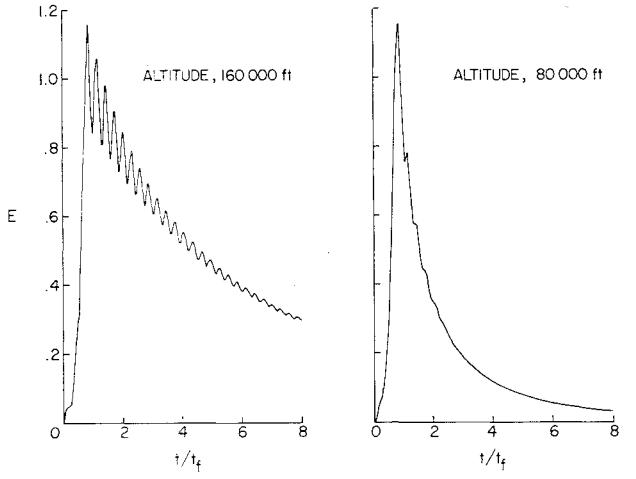

Fig. 3 Normalized force histories, E, for different depolyment altitudes.

The force on the payload can be obtained by multiplying Eqs. (3) by $-k$. This force can be expressed as $(-kq_sC_DS_o/m_1\omega^2)E$, which reduces to $-q_sC_DS_oE$ for $m_2 \gg m_1$. E is then a force normalized to the steady load and can be obtained from Eqs. (3), once the exponent n is specified and the integration is performed. Table 1 lists expressions for E with n varying from 1–4. The maximum value of E (or the load amplification factor, M) can be determined after setting $dE/dt = 0$ and obtaining those maximizing values of t for various values of t_f. This has been done for the cases in Table 1 and it was found that M occurs shortly after full inflation (at approximately $t_f + T/4$). The load amplification factors are presented in Fig. 2 as a function of the ratio of filling time to the natural oscillation period of the elastic system. From Fig. 2 it is seen that M varies between 1 and 2 and is generally decreasing with increasing t_f/T. For $t_f/T > 2$ and $n > 1$, M varies approximately as $1 + (nT/2\pi t_f)$. Therefore, when the filling time is very short or when the natural period of oscillation is relatively long (i.e., low value of k), elasticity can result in significant opening load amplification. (Although the present analysis indicates that suspension lines with a higher spring constant can reduce opening load amplification, Ref. 1 indicates that stiffer lines increase snatch force. Hence, both opening load and snatch force should be considered, when designing a parachute system for a specific application.)

Another interesting result obtained from the elastic model is the character of the load history immediately following full inflation. Here the assumption of $\dot{x}_1$ (or $\dot{x}_2$) being nearly constant cannot be made since the system will be rapidly decelerating due to the drag provided by the fully inflated canopy. Instead, one can now assume that the drag area maintains a constant value. By setting $\dot{x}_2/\dot{x}_1 = (1 + \varphi)$, where $\varphi \ll 1$ a dimensionless parameter, Eqs. (1) can be combined to yield

$$\ddot{\xi} - (C_DS_o\rho\dot{\xi}/2m_1\varphi^2)\dot{\xi} + \omega^2\xi = 0 \qquad (4)$$

Hence, this change in assumptions produces an equation different from Eq. (2). For $\dot{\xi} < 0$, the parachute is closing on the payload and the second term in Eq. (4) represents nonlinear damping of the spring-mass system. For $\dot{\xi} > 0$, the parachute is increasing its separation distance from the payload and energy is being put back into the system. For any single cycle oscillation, energy is added and then dissipated. The net result is an oscillation about the steady drag loading history. The amplitude of oscillation will depend on the "damping" term. One obvious consequence of this is that for a given parachute system the amount of "damping" decreases as the density decreases. Hence, one could expect oscillating load histories initiated by the inflation process to persist at high altitude even when the parachute drag area remains steady. Numerical solutions of Eqs. (1) were obtained for identical parachute systems, operating under nearly infinite mass conditions, at the same dynamic pressure but different altitudes. The resulting payload force histories were normalized to the steady load and are presented in Fig. 3 as a function of the ratio of time to filling time. Note for both cases that the opening load is amplified, as predicted by the earlier analysis. Also, note that the load oscillation following full inflation for the higher altitude case has less "damping" than the lower altitude case, as predicted by the later analysis. This altitude or density effect can be noteworthy above about 80,000 ft. For parachute tests at lower altitudes, the elastic system will have high "damping." And load oscillation due to suspension line elasticity would not be expected.

In general, when the drag area does not remain constant following full inflation, load oscillations can be much more severe than that indicated in Fig. 3. This was the case for the flight test reported in Ref. 2, where it was shown that the elastic model could provide a good reproduction of the payload force time history.

Conclusions

Using a two-body spring-mass system to analyze parachute loads, the following conclusions can be stated:

1) For infinite mass parachute deployments, suspension line elasticity can result in an amplification of the opening load. For those cases where the growth in drag area during inflation is proportional to $(t/t_f)^n$, the magnitude of the effect can be approximated by $1 + (nT/2\pi t_f)$.

2) For parachute deployments at high altitude (above about 80,000 ft), oscillating load histories initiated by the inflation process will persist as a result of reduced "damping" due to the small value of atmospheric density.

References

[1] "Performance of and Design Criteria for Deployable Aerodynamic Decelerators," ASD-TR-61-579, Dec. 1963, U.S. Air Force, pp. 164, 143.

[2] Eckstrom, C. V. and Preisser, J. S., "Flight Test of a 40-Foot-Nominal Diameter Disk-Gap-Band Parachute Deployed at a Mach Number of 2.72 and a Dynamic Pressure of 9.7 Pounds Per Square Foot," TM X-1623, 1968, NASA.

[3] Jacobsen, L. S. and Ayre, R. S., *Engineering Vibrations*, Chap. 4, McGraw-Hill, New York, 1958.

Technical Comment

Erratum: "Solar Deflection of Thin-Walled Cylindrical, Extendible Structures"

Robert J. Eby* and Robert D. Karam†
Fairchild Hiller Corporation, Germantown, Md.

[J. Spacecraft Rockets, 7, 577–581, (1970)]

αT^4 and αT^4_{av} in Eqs. (6) and (10) should read σT^4 and σT^4_{av}, respectively. σ is the Stefan-Boltzmann constant. Similarly, the α in Eq. (15) should be σ. The same error occurs in the example; thus, $\sigma T^4_{av} = 233.43$ and $\sigma T^3_{av} = 0.384$.

Received June 18, 1970.

* Manager, Thermal Control, Space and Electronics Systems Division.

† Principal Engineer, Thermal Control, Space and Electronics Division.